

V.N. Zakharov, G.N. Feyt, O.N. Malinnikova, A.P. Averin
ROCKS' VIBRATORY ENERGY IN THE AREA OF MOUNTAIN WORKING ON
THE ASSUMPTION OF UNDERGROUND COAL MINING.

Research Institute of Comprehensive Exploitation Of Mineral Resources, Russian Academy of Sciences
 Russia, 111020, Moscow, Krukovskiy tunic, 4
 Tel. (495) 360-07-35, Fax. (495) 360-89-60

The authors have investigated features, forecasting characteristics and interdependence between development of geomechanical processes and acoustic vibration of coal bed and country rock in critical area of formation in the process of forming hazard's sites of gas-dynamic phenomena. It has been discovered that in the certain combination of physical and mechanical properties of rocks, amplitude-frequency spectrum of vibration source and starting strained and deformed state oscillation process in coal massif can turn into self-vibrating and resonant mode and activate rock burst or sudden coal or gas blowout.

V.O. Vakhnenko¹, O.O. Vakhnenko², J.A. TenCate³, T.J. Shankland³
THE DYNAMICS OF A SANDSTONE BAR UNDER RESONANCE LOADING

¹Subbotin Institute of Geophysics, NAS Ukraine
 Ukraine, 63-B Bohdan Khmel'nyts'ky Street, Kyiv 01054
 E-mail: vakhnenko@ukr.net

²Bogolyubov Institute for Theoretical Physics, NAS Ukraine
 Ukraine, 14-B Metrologichna Street, Kyiv 03143
 E-mail: vakhnenko@bitp.kiev.ua

³Los Alamos National Laboratory
 USA, Los Alamos, New Mexico 87545
 E-mail: tencate@lanl.gov, shanklan@lanl.gov

We propose a closed-form scheme that reproduces a wide class of nonlinear and hysteretic effects exhibited by sedimentary rocks in longitudinal bar resonance. In particular, we correctly describe: hysteretic behaviour of a resonance curve on both its upward and downward slopes; linear softening of resonant frequency with increase of driving level; gradual (almost logarithmic) recovery (increase) of resonant frequency after large dynamical strains; and temporal relaxation of response amplitude at fixed frequency. Starting with a suggested model, we predict the dynamical realization of end-point memory in resonating bar experiments with a cyclic frequency protocol. The effect we describe and simulate is defined as the memory of previous maximum amplitude of alternating stress and manifested in the form of small hysteretic loops inside the main hysteretic loop on the resonance curve. These theoretical findings were confirmed experimentally at Los Alamos National Laboratory.

Sedimentary rocks, particularly sandstones, are distinguished by their grain structure in which each grain is much harder than the intergrain cementation material [1]. The peculiarities of grain and pore structures give rise to a variety of remarkable nonlinear mechanical properties demonstrated by rocks, both at quasistatic and alternating dynamic loading [1-4]. Thus, the hysteresis earlier established for the stress-strain relation in samples subjected to quasistatic loading-unloading cycles has also been discovered for the relation between acceleration amplitude and driving frequency in bar-shaped samples subjected to an alternating external drive that is frequency-swept through resonance. At strong drive levels there is an unusual, almost linear decrease of resonant frequency with strain amplitude, and there are long-term relaxation phenomena such as nearly logarithmic recovery (increase) of resonant frequency after the large conditioning drive has been removed.

In this report we present a short sketch of a model [5,6] for explaining numerous experimental observations seen in forced longitudinal oscillations of sandstone bars. According to our theory a broad set of experimental data can be understood as various aspects of the same internally consistent pattern [5,6]. A reliable probing method widely applied in resonant bar experiments is to drive a horizontally suspended cylindrical sample with a piezoelectric force transducer cemented between one end of the sample and a massive backload, and to simultaneously measure the sample response with a low-mass accelerometer attached to the opposite end of the bar [2,4]. The evolution equation for the field of bar longitudinal displacements u as applied to above experimental configuration we write as follows

$$\rho \frac{\partial^2 u}{\partial t^2} = \frac{\partial \sigma}{\partial x} + \frac{\partial}{\partial x} \left[\frac{\partial \mathfrak{S}}{\partial (\partial^2 u / \partial x \partial t)} \right]. \quad (1)$$

Here we use the Stokes internal friction associated with the dissipative function $\mathfrak{S} = (\gamma/2)[\partial^2 u / \partial x \partial t]^2$.

The quantities ρ and γ are, respectively, mean density of sandstone and coefficient of internal friction. The stress-strain relation ($\sigma - \partial u / \partial x$) we adopt in the form

$$\sigma = \frac{E \operatorname{sech} \eta}{(r-a) [\cosh \eta \partial u / \partial x + 1]^{a+1}} - \frac{E \operatorname{sech} \eta}{(r-a) [\cosh \eta \partial u / \partial x + 1]^{r+1}}, \quad (2)$$

which for $r > a > 0$ allows us to suppress the bar compressibility at strain $\partial u / \partial x$ tending toward $+0 - \operatorname{sech} \eta$. Thus, the parameter $\cosh \eta$ is assigned for a typical distance between the centers of neighboring grains divided by the typical thickness of intergrain cementation contact.

The indirect effect of strain on Young's modulus E , as mediated by the concentration c of ruptured intergrain cohesive bonds, is incorporated in our theory as the main source of all non-trivial phenomena. We introduce a phenomenological relationship between defect concentration c and Young's modulus. Intuition suggests that E must be some monotonically decreasing function of c , which can be expanded in a power series with respect to a small deviation of c from its unstrained equilibrium value c_0 . To lowest informative approximation we have

$$E = (1 - c / c_{cr}) E_+. \quad (3)$$

Here c_{cr} and E_+ are the critical concentration of defects and the maximum possible value of Young's modulus, respectively. The equilibrium concentration of defects c_σ associated with a stress σ is given by

$$c_\sigma = c_0 \exp(\nu \sigma / kT), \quad (4)$$

where the parameter $\nu > 0$ characterizes the intensity of dilatation. Although formula (4) should supposedly be applicable to the ensemble of microscopic defects in crystals, it was derived in the framework of continuum thermodynamic theory that does not actually need any specification of either the typical size of an elementary defect or the particular structure of the crystalline matrix. For this reason we believe it should also work for an ensemble of mesoscopic defects in consolidated materials, provided that for a single defect we understand some elementary rupture of intergrain cohesion. The approximate functional dependence of c_0 on temperature T and water saturation s based on experimental data was treated in [5,6].

In order to achieve reliable consistency between theory and experiment we have used the concept of blended kinetics, which finds more-or-less natural physical justification in consolidated materials [6]. The idea presents the actual concentration of defects c as some reasonable superposition of constituent concentrations g , where each particular g obeys rather simple kinetics. Specifically, we take the constituent concentration g to be governed by the kinetic equation:

$$\partial g / \partial t = -[\mu \theta(g - g_\sigma) + \nu \theta(g_\sigma - g)](g - g_\sigma). \quad (5)$$

Here $\mu = \mu_0 \exp(-U / kT)$ and $\nu = \nu_0 \exp(-U / kT)$ are the rates of defect annihilation and defect creation, respectively, and $\theta(z)$ designates the Heaviside step function. A huge disparity $\nu_0 \gg \mu_0$ between the priming rates (attack frequencies) ν_0 and μ_0 is assumed, notwithstanding the native cohesive properties of cementation material. Typical resonant response experiments [1-2,4] correspond to forced longitudinal vibration of a bar, which we associate with the boundary conditions:

$$u(x=0|t) = D(t) \cos(\varphi + \int_0^t d\tau \omega(\tau)), \quad \sigma(x=L|t) + \gamma \frac{\partial^2 u}{\partial x \partial t}(x=L|t) = 0, \quad (6)$$

where L is sample length, and $D(t)$ is driving amplitude. Initial conditions are

$$u(x|t=0) = 0, \quad \frac{\partial u}{\partial t}(x|t=0) = 0, \quad g(x|t=0) = c_0. \quad (7)$$

Computer modeling of nonlinear and slow dynamics effects was performed in the vicinity of the resonance frequency $f_0(2)$, which we choose to be the second frequency ($l=2$) in the fundamental set,

$$f_0(l) = \frac{2l-1}{4L} \sqrt{(1 - c_0 / c_{cr}) E_+ / \rho} \quad (l=1, 2, 3, \dots). \quad (8)$$

Figure 1 shows typical resonance curves, i.e., dependences of response amplitudes R (calculated at $x=L$) on drive frequency $f = \omega/2\pi$, at successively higher drive amplitudes D . Solid lines correspond to conditioned resonance curves calculated after two frequency sweeps were performed at each driving level in order to achieve repeatable hysteretic curves. The dashed line illustrates an unconditioned curve obtained without any preliminary conditioning. Arrows on the three highest curves indicate sweep directions. To improve the illustration, results of the computer simulations were adapted to experimental conditions appropriate to the data obtained by TenCate and Shankland for Berea sandstone [2]. In particular, $L = 0.3\text{ m}$, $f_0(2) = 3920\text{ Hz}$, $\nu E_+ / k \cosh \eta = 275\text{ K}$, $\cosh \eta = 2300$, $a = 2$, $r = 4$.

The shift of resonance frequency as a function of drive amplitude D was found to follow the almost linear dependence typical of materials with nonclassical nonlinear response, i.e., materials that possess all the basic features of slow dynamics (see [5,6] for more details). Figure 2 shows the gradual recovery of resonant frequency f_r to its maximum limiting value f_0 after the bar has been subjected to high amplitude conditioning and conditioning was stopped. We clearly see the very wide time interval $10 \leq (t - t_c)/t_0 \leq 1000$ of logarithmic recovery of the resonant frequency, in complete agreement with experimental results [4]. Here t_c is the moment when conditioning switches off and $t_0 = 1\text{ s}$ is the time scaling constant. Curves $j = 1, 2, 3$ on Fig. 2 correspond to successively high water saturations $s_j = 0.05(2j - 1)$.

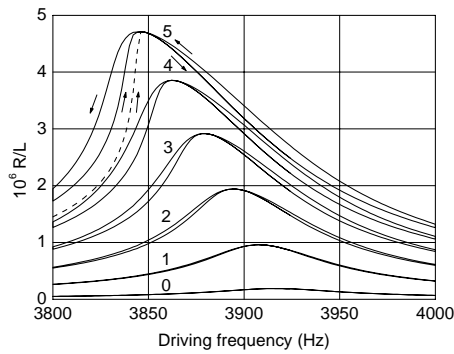


Figure 1. Resonance curves $j = 0, 1, 2, 3, 4, 5$ at successively higher driving amplitudes $D_j = 3.8(j + 0.2\delta_{j0}) 10^{-8} L$. The time to sweep back and forth within the frequency interval $3700 - 4100\text{ Hz}$ is chosen to be 120 s .

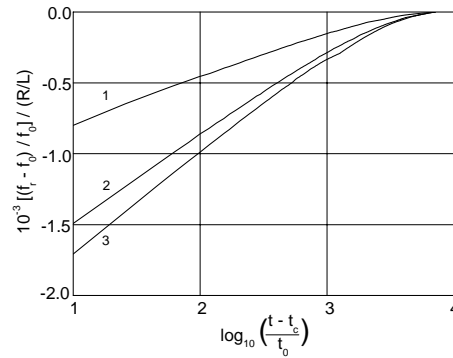


Figure 2. Time-dependent recovery of resonant frequency f_r to its asymptotic value f_0 . The frequency shift $f_r - f_0$ is normalized by both the asymptotic frequency f_0 and the unitless response amplitude R/L attained at conditioning resonance.

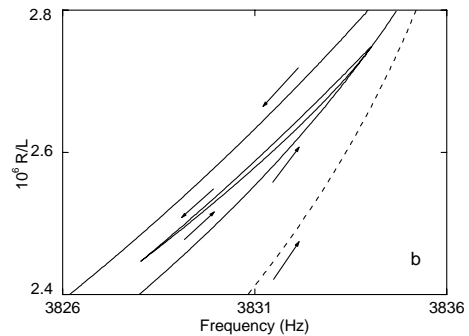
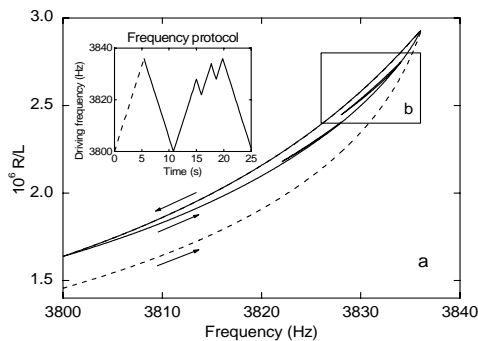


Figure 3. Manifestation of end-point memory in dynamic response with a multiply-reversed frequency protocol.

Hence, the system of the equations (1-5) enables us to describe correctly a wide class of experimental facts concerning the unusual dynamical behaviour of such mesoscopically inhomogeneous media as sandstones [4-6]. Moreover, as it is shown below, we have predicted the phenomenon of hysteresis with end-point memory in its essentially dynamical hypostasis [6]. These theoretical findings were confirmed experimentally in Los Alamos National Laboratory.

The question of whether an effect similar to the end-point (discrete) memory that is observed in quasi-static experiments with a multiply-reversed loading-unloading protocol (see refs. [7-9] and references there) could also be seen in resonating bar experiments with a multiply-reversed frequency protocol has been raised in [6] and was first examined theoretically. The graphical results of this investigation are presented in Fig. 3 (see also Fig. 16 in [6]). The model constants are given in [6]. One of the features of dynamical end-point memory, defined here as the memory of the previous maximum amplitude of alternating stress, is seen as small loops inside the major loop. The starting and final points of each small loop coincide, which is typical of end-point memory.

Following the theoretical results, shown in Fig. 3, we performed experimental measurements to verify our prediction. The sample bar was a Fontainebleau sandstone and the drive level produced a calculated strain of about $2 \cdot 10^{-6}$ at the peak. Figure 4 shows the low frequency sides of resonance curves that correspond to the frequency protocol given on inset of Fig. 4. We clearly see that the beginning and end of each inner loop coincide, i.e., a major feature of end-point memory.

The experimental results for the Fontainebleau sandstone shown in Fig. 4 were reproduced by using our model equations though with constants (including a state equation) developed for Berea sandstone [5, 6]. We note the good qualitative agreement between the experimental (Fig. 4) and the theoretical (Fig. 5) curves suggesting that our physical model is appropriate for both sandstones.

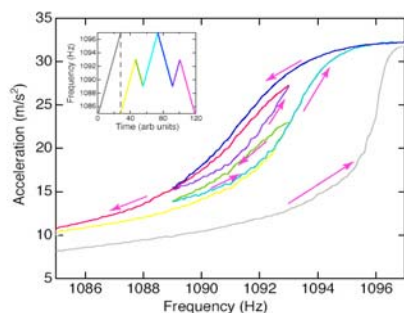


Figure 4. Figure 4. The low frequency sides of experimental resonance curves for Fontainebleau sandstone.

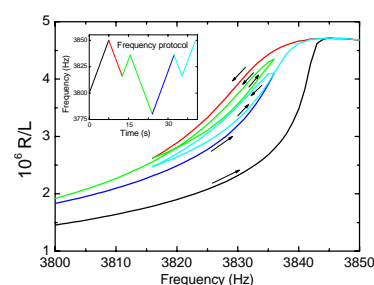


Figure 5. The low frequency sides of the resonance curves calculated for Berea sandstone.

J.A.T. and T.J.S. thank the Geosciences Research Program, Office of Basic Energy Sciences of the U.S. Department of Energy for sustained assistance and also Institutional Funding support from the Los Alamos' LDRD program.

REFERENCES

1. Guyer R.A., Johnson P.A. Nonlinear mesoscopic elasticity: Evidence for a new class of materials // *Physics Today*. 1999. V.52. P.30-35.
2. TenCate J.A., Shankland T.J. Slow dynamics in the nonlinear elastic response of Berea sandstone // *Geophys. Res. Lett.* 1996. V. 23. P.3019-3022.
3. Van Den Abeele K., Carmeliet J., Johnson P., Zinszner B. The influence of water saturation on the nonlinear mesoscopic response of earth materials, and the implications to the mechanism of nonlinearity // *Journal of Geophysical Research*. 2002. V.107. P.10,1029-10,1040.
4. TenCate J.A., Smith E., Guyer R.A. Universal slow dynamics in granular solids // *Phys. Rev. Lett.* 2000. V.85. P.1020-1024.
5. Vakhnenko O.O., Vakhnenko V.O., Shankland T.J., TenCate J.A. Strain-induced kinetics of intergrain defects as the mechanism of slow dynamics in the nonlinear resonant response of humid sandstone bars // *Phys. Rev. E*. 2004. V.70, Rapid communication, 015602(4).
6. Vakhnenko O.O., Vakhnenko V.O., Shankland T.J. Soft-ratchet modelling of end-point memory in the nonlinear resonant response of sedimentary rocks // *Phys. Rev. B*. 2005. V.71. P.174103(14).
7. Guyer R.A., McCall K.R., Boitnott G.N., Hilbert Jr. L.B., Plona T.J. Quantitative use of Preisach-Mayergoyz space to find static and dynamic elastic moduli in rock // *J. Geophys. Res.* 1997. V.102. P.5281-5293.
8. Darling T.W., TenCate J.A., Brown D.W., Clausen B., Vogel S.C. Neutron diffraction study of the contribution of grain contacts to nonlinear stress-strain behavior // *Geophys. Res. Lett.* 2004. V.31. P. L16604(4).
9. Vakhnenko V.O., Vakhnenko O.O., TenCate J.A., Shankland T.J. Modeling of stress-strain dependences for Berea sandstone under quasistatic loading // *Phys. Rev. B*. 2007. V.76. P.184108 (8).